11-1996

Fundamental limits to imaging resolution for focused ion beams

Jon Orloff

L. W. Swanson

Mark Utlaut
University of Portland, utlaut@up.edu

Fundamental limits to imaging resolution for focused ion beams

Jon Orloff
Department of Electrical Engineering and Institute for Plasma Research, University of Maryland, College Park, Maryland 20742-3511

L. W. Swanson
FEI Co., Hillsboro, Oregon 97124

M. Utlaut[a)]
Department of Physics, University of Portland, Portland, Oregon 97203

(Received 28 May 1996; accepted 12 August 1996)

This article investigates the limitations on the formation of focused ion beam images from secondary electrons. We use the notion of the information content of an image to account for the effects of resolution, contrast, and signal-to-noise ratio and show that there is a competition between the rate at which small features are sputtered away by the primary beam and the rate of collection of secondary electrons. We find that for small features, sputtering is the limit to imaging resolution, and that for extended small features (e.g., layered structures), rearrangement, redeposition, and differential sputtering rates may limit the resolution in some cases. © *1996 American Vacuum Society.*

I. INTRODUCTION

The use of liquid metal ion sources has provided a basis for the high performance of focused ion beam (FIB) systems. Beam sizes under 10 nm with current densities of 1–10 A/cm^2 are now routinely obtained. The FIB system has found extensive use in the last decade, especially in various aspects of integrated circuit (IC) fabrication processes. The aspects of the FIB which are important are its ability to remove (via sputtering) and add (via ion induced deposition) materials at sub-micron dimensions. FIB systems are now used to perform a variety of critical tasks such as design modification, failure analysis, defect characterization, and process control functions.

FIB systems are now being used as scanning ion microscopes (SIM) to inspect defects, layer thickness, or grain sizes that have been exposed by FIB cross-sectioning techniques. In several situations, FIB imaging is preferred over higher resolution scanning electron microscope (SEM) imaging because there are different contrast mechanisms available with either secondary electron or secondary ion detection. As IC feature sizes continue to be reduced, it has become desirable to have FIB systems resolve sub-10 nm dimensions. It is of interest to understand how far imaging resolution can be extended before fundamental limits are reached. We consider here only FIB induced secondary electron images since, in general, the secondary ion yield is orders of magnitude less than the secondary electron yield.

II. IMAGE FORMATION AND INFORMATION THEORY

There are three quantities which are inter-related that determine the quality of an image: resolution, contrast, and signal-to-noise. In order to form an image of acceptable quality, all three must be present in sufficient quantity. In 1879, Rayleigh[1] proposed a definition of resolution for light, which although stated for diffraction limited systems, had the essence of what is meant by resolution: namely the ability just to distinguish two objects spatially. There is implicit in this definition the notion that there must be some discernible difference in contrast between the objects and the space between them and that there is sufficient signal-to-noise. Contrast is defined in terms of intensity as

$$C=\frac{I_{\max}-I_{\min}}{I_{\max}+I_{\min}}. \tag{1}$$

Signal-to-noise is defined as the ratio of the rms signal to the rms fluctuations due to noise.

This notion is quantified by determining the functional dependence of the contrast in terms of the spatial frequencies f in the image, and is known as the modulation transfer function (MTF) or the optical transfer function (OTF). The OTF of an optical system is the Fourier transform of the current density distribution.[2] Orloff[3] has shown the effects of optical aberrations on the OTF. If the OTF is normalized to unity at $f=0$, the Rayleigh criterion corresponds to a contrast level of 10%, so that $f_{10\%}{}^{-1}=D$ is the resolution obtainable.[4] Figure 1 shows a FIB secondary electron image of graphite obtained on an FEI FIB 800. The contrast response as a function of spatial frequency was determined in several locations where two ridges come together by measuring C as a function of their spatial separation. The results of that measurement are shown in Fig. 2. Since the Rayleigh criterion corresponds to a contrast level of ~10%, it can be seen that the resolution is ~5 nm. This method of measuring resolution, although straightforward, is tedious, and does not lend itself to easy analysis by computer.

The signal-to-noise ratio of a system must be good enough to detect a given level of contrast. If the signal-to-noise ratio K is limited by the primary beam, which we as-

[a)]Electronic mail: marku@up.edu

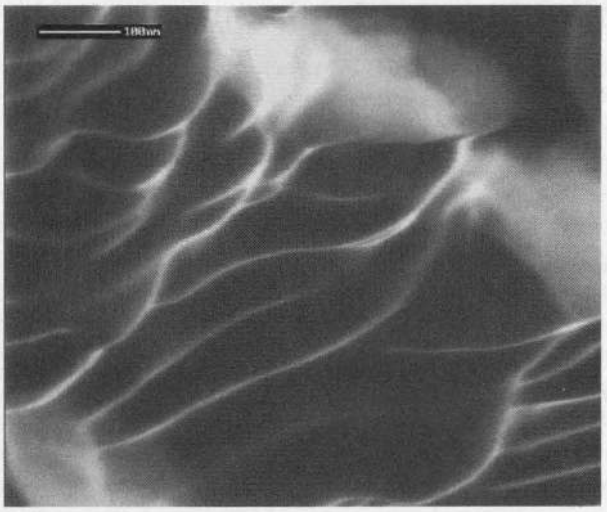

FIG. 1. Secondary electron image of graphite obtained with an FEI FIB 800.

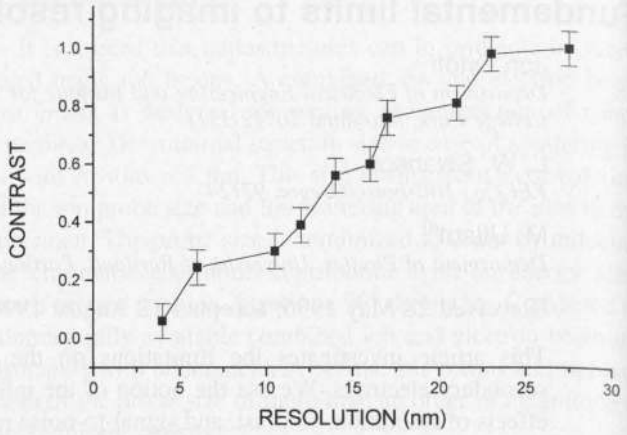

FIG. 2. Contrast modulation measured from selected regions of Fig. 1. The resolution is defined for any value of contrast. The Rayleigh criterion corresponds to a contrast level of 10%.

sume is Poisson distributed, then for each pixel in the image, $K \propto N_i^{1/2} \propto t_d^{1/2}$, where N_i is the number of primary ions/pixel and t_d is the beam dwell time per pixel. Thus, in order to increase K, N_i and t_d must also increase. Figure 3 shows the effect of t_d on K.

The information content of an image is defined as[5]

$$H = \frac{\pi^2}{\ln 2} \int_0^2 \ln(1 + K|\mathrm{OTF}(\overline{\nu})|^2)\, \overline{\nu} d\overline{\nu}, \tag{2}$$

where $\overline{\nu} = \nu MD$ is the normalized spatial frequency and M and D are the magnification and radius of the source. It can be seen that in order to maximize H for a given source and magnification, the area under the OTF curve should be maxi-

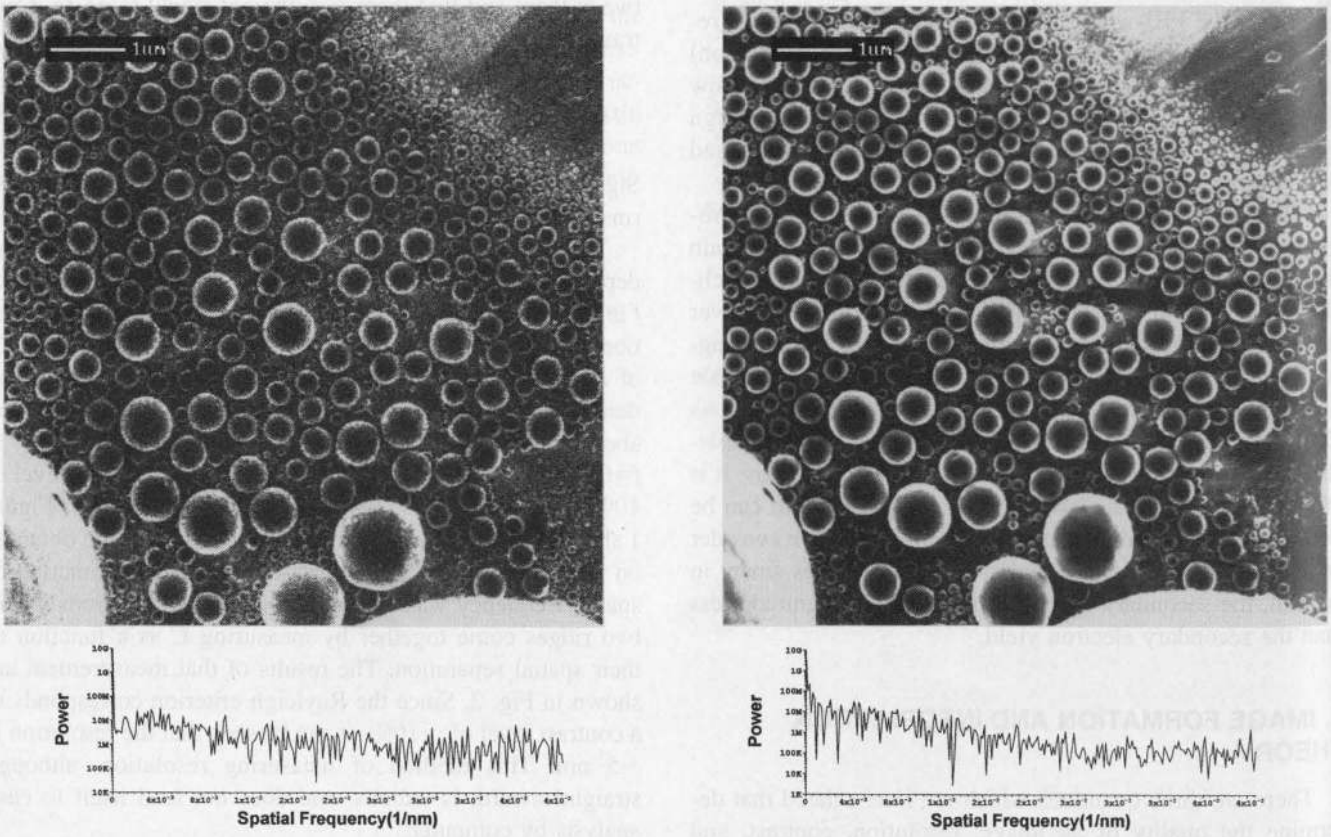

FIG. 3. Secondary electron images of evaporated Sn spheres. The dwell times were 4.8μs and 160μs, the primary ion beam current was 1pA of Ga^+. Note the higher resolution with increasing dwell time due to increased signal-to-noise. Below each figure is the power spectrum of the same line scan for each image.

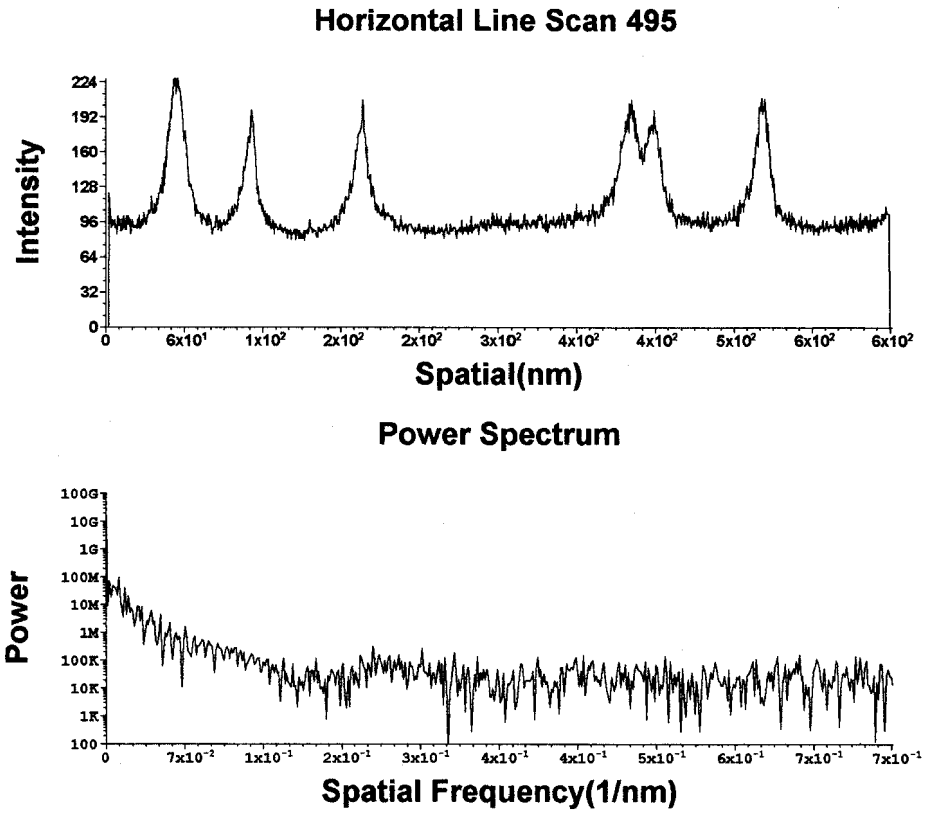

FIG. 4. Power spectrum of a line in Fig. 1. The inverse of the spatial frequency where the signal falls to the noise is ~5 nm.

mized (aberrations minimized) and K should be maximized. This technique can be used to measure the resolution of an image, by computing the power spectrum, and finding the inverse of the spatial frequency where the signal reaches the noise level of the system.[4] Figure 3 also shows the computed power spectra of the same line scan of each image. Fig. 4 shows the power spectrum of one line scan of the image of graphite in Fig. 1. Again we see that the resolution is ~5 nm. This method of measuring resolution is easy to use and objective.

There is a practical maximum that K needs to be based on the response of the human eye. The normal human eye responds to the logarithm of intensities (Weber–Fechner law), and can perceive 20–30 gray levels.[6] A value of K for a very good image is about 20.[7] Most digital imaging systems now work with 8-bit (256) gray levels, which is far beyond what the eye is capable of perceiving. In addition, an increased number of gray levels requires more secondary electrons, and causes more sample erosion. Since the eye cannot perceive all of these levels, it is possible that there is wasted information.

III. SPUTTERING

In the SEM, the fundamental limit of resolution is optical (column aberrations, source brightness) for materials which are not altered by the beam. The same limit exists for the FIB, but due to the continuous removal of the sample by sputtering, another fundamental limit exists which is the competition between the rate of sputtering of the sample and the rate at which information (generally secondary electrons) can be collected.

The sputter rate of sample features depends on both the sample and primary ion species. The sputter yield Y (sputtered atoms/primary ion) depends on the transfer of primary ion momentum and energy to the target atoms, so that both the mass of the primary ion and sputtered species as well as the sublimation energy of the target need to be considered.

The total number of sample particles sputtered in one raster scan of the ion beam is

$$N = \frac{V\rho N_0}{A} = Y N_i N_l^2, \tag{3}$$

where V is the total volume removed, ρ and A are the target density and atomic or molecular weight, N_i is the number of ions per pixel onto the target, and N_l is the number of pixels per line. The total volume removed in one raster scan is

$$V = \frac{Y N_i N_l^2 A}{\rho N_0} \tag{4}$$

and can be related to the raster size and magnification as

$$V = l^2 z = \frac{L^2 z}{M^2}, \tag{5}$$

TABLE I. Calculated values of Y and M from experimental values of S, using $K=20$ $N_i=1024$, $L=30$ cm, and $\delta=1.5$ for the elements, and $\delta=2$ for the compounds.

Substrate	Y (atoms/ion)	S (μm^3/nC)	Mag. (kX)
C (diamond)	2.7	0.18	133
Si	2.2	0.27	117
Al	2.9	0.30	112
Ti	3.3	0.37	104
Cr	1.3	0.10	162
Fe	3.9	0.29	114
Ni	2.0	0.14	145
Cu	3.4	0.25	120
Mo	1.2	0.12	153
Ta	2.8	0.32	110
W	1.2	0.12	153
Au	14.1	1.5	66
MgO	1.3	0.15	147
SiO_2	0.6	0.24	134
Al_2O_3	0.3	0.08	181
TiO	1.1	0.15	147
Si_3N_4	0.5	0.20	133
TiN	1.2	0.15	147
Fe_2O_3	0.8	0.25	124
GaAs	2.1	0.61	92

where l is the raster size on the sample, M is the magnification, z is the depth of sample removed per scan, and L is the viewing screen size.

The beam can overlap itself during the scan. The overlap ω is defined by $\omega=(D-s)/D$, where D is the beam diameter, and s is the scan step size. A maximum square raster of $L=W$ then gives

$$\omega=1-\frac{L}{MDN_l}, \tag{6}$$

and assuming a flat distribution beam shape of diameter D, then with $\Omega=1-\omega$,

$$zD^2=\frac{YAN_i}{\Omega^2\rho N_0}. \tag{7}$$

This can be rewritten in terms of the sputtering sensitivity $S(\mu\text{m}^3/\text{nC})$ which is a function of sample parameters only as

$$zD^2=\frac{SN_ie}{\Omega^2} \tag{8}$$

with

$$S=\frac{YA}{\rho N_0 e}. \tag{9}$$

Table I lists values of S measured by Leslie[8] and Stark *et al.*[9] for various substrates for Ga^+ at 30 kV. These values were obtained by milling square, low aspect ratio holes with a known total charge of Ga^+ ions, and then measuring their volume with an AFM. Typically values for most materials of S are between 0.1 and 0.3 μm^3/nC. Also shown in Table I are calculated values of Y for the substrates.

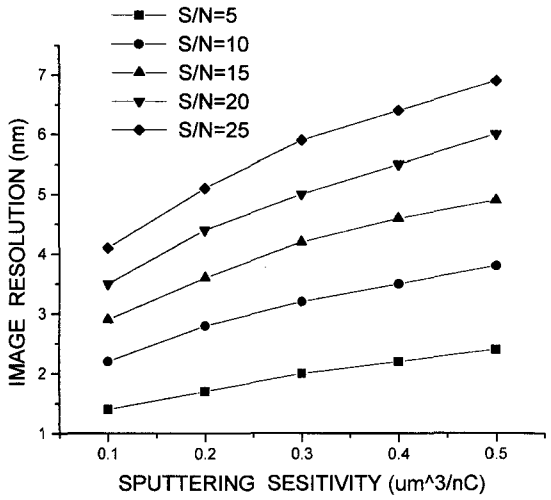

FIG. 5. Plot of the calculated values of $D_{\min}$ as a function of sputter sensitivity.

Assuming that all secondary electrons from the sample are collected by the detector, it has been shown that assuming both the primary ion beam and generated secondary electrons are Poisson distributed and that there are no other sources of noise in the system, that the signal-to-noise K is[10]

$$K=\sqrt{\frac{N_i\delta}{1+\delta}}, \tag{10}$$

where δ is the secondary electron yield due to the ion beam. A "noise bottleneck"[10] will occur in the primary beam if $\delta>1$ and in the secondary electron current if $\delta<1$. Equation (7) can then be written as

$$zD^2=\frac{eSK^2(1+\delta)}{\Omega^2\delta}. \tag{11}$$

This shows the importance of operating at a maximum value of Ω (minimum value of ω) in order to minimize the volume of sample removed during image formation for a given value of K.

Experience in accumulating many high resolution secondary electron FIB images from a variety of samples has shown that $N_i=700\pm200$ is required for an image of a flat surface. This yields an image with $K=21\pm3$ for $\delta=2$. Assuming now that there is a feature such that $z=D$, we find that for the above values of K and δ, and with $\Omega=0.5$ that

$$D_{\min}=4.23\times10^{-7}S^{1/3}. \tag{12}$$

We see that for a desired level of K, and for fixed Ω and δ that the ultimate resolution is determined by the rate of sputtering for the small feature. Of course, if one is willing to sacrifice signal-to-noise, the minimum detectable feature would be smaller. $K=5$ is about the minimum that can be tolerated, and then

$$D_{\min}=2.4\times10^{-8}\,S^{1/3}. \tag{13}$$

Values of $D_{\min}$ are shown in Fig. 5 for various levels of K assuming $\Omega=0.5$ and $\delta=1.5$.

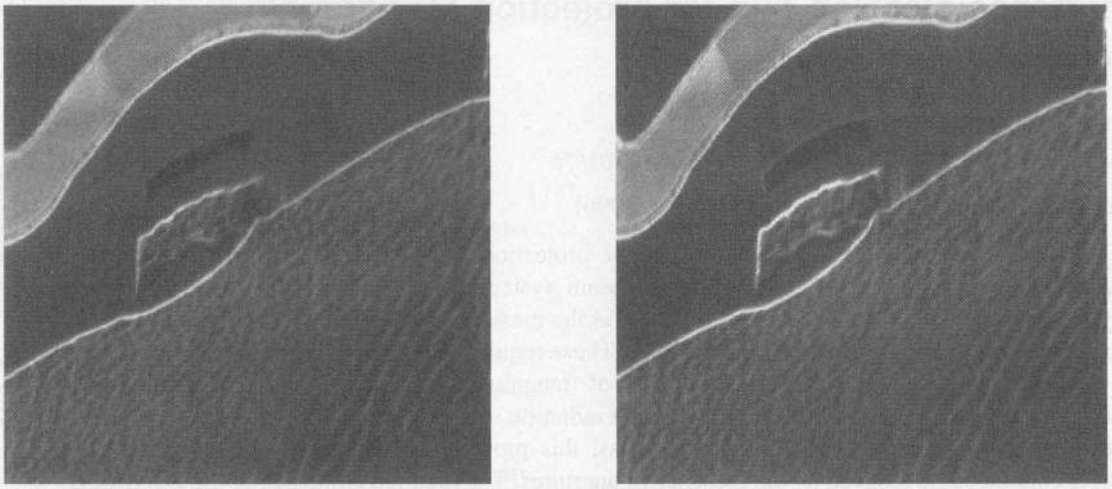

FIG. 6. Secondary electron images of a corner cross section of a semiconductor obtained with an FEI FIB 800. Both were imaged with a 1 pA beam with a dwell time of 160 μs. The right image had a dose ~4320 more Ga^+ ions. The full scale of each image is 2.85 μm.

A practical value for operation is $\omega=0.5$, so that the maximum allowable magnification is

$$M=\frac{2L}{DN_l}. \tag{14}$$

For typical viewing monitors used with FIB systems, $L \approx 30$ cm and for typical hardcopy printouts, $L \approx 15$ cm and $N_l=1024$ pixels/line. Included in Table I is the maximum magnification as a function of sputtering sensitivity.

IV. EXTENDED STRUCTURES

One of the major uses for FIB is for cross-sectioning structures.[11] After the cross-sectioning has occurred and the structure is viewed in the FIB, the above analysis pertains only to small structures in the cross section. For extended features in layered structures, the fundamental limit to resolution is no longer signal limited due to a finite volume of material, but rather to the effects of rearrangement, redeposition, and differential sputtering rates. Rearrangement will cause the loss of channeling contrast as the channels are blocked.[12] Redeposition will smear features as material is spread over the surface. Differential sputtering rates result in non-uniform erosion, leading to topographic contrast which may be difficult to interpret, as well as leading to enhanced redeposition effects in pitted areas. Figure 6 shows a small area of a corner cross section of a semiconductor after several scans. It is evident that under these conditions that there appears to be no significant loss of resolution or contrast. The same features at the 5–10 nm level are clearly visible in images, the right image after a dose of ~4320 Ga^+ ions/pixel.

V. CONCLUSIONS

It appears that the imaging resolution of the FIB for small particles and fine structures is limited by the differential rate of sputtering and secondary electron collection, and depending upon the signal-to-noise ratio required in an image is of the order of a few nm. For some extended fine structures (layered), imaging resolution is limited by rearrangement, redeposition, and differential sputtering rates for the materials present. FIB systems are now at the point where sputtering seems to be the fundamental limit, and it appears that to go to higher resolution with sufficient signal-to-noise will require sources of low mass ions (e.g., H^+) reduce the sputtering yield.

ACKNOWLEDGMENTS

One author (J.O.) is grateful to the U.S. Department of Defense Microelectronics Research Laboratory for support (Contract No. MDA 904-94-H2039). Another author (M.U.) acknowledges the support of a Murdock Charitable Trust grant to the University of Portland.

[1]Lord Rayleigh, Philos. Mag. **8**, 261 (1879).
[2]J. Orloff, Rev. Sci. Instrum. **64**, 1105 (1993).
[3]J. Orloff, SPIE Proc. **3125**, 92 (1995).
[4]M. Sato and J. Orloff, Ultramicroscopy **41**, 181 (1992).
[5]P. B. Felleget and E. H. Linfoot, Philos. Trans. A **247**, 369 (1955).
[6]T. M. Cornsweet, *Visual Perception* (Academic, New York, 1970).
[7]The best photographs have at most 30 levels.
[8]A. Leslie, in Proceedings of the 5th European Symposium on Reliability of Electron Devices, Failure Physics and Analysis, Int. J. Qual. Reliab. Eng. **14**, 43 (1994).
[9]T. Stark, B. Shedd, J. Bitarelli, D. Griffis, and P. Russell, J. Vac. Sci. Technol. B **13**, 282 (1995).
[10]O. C. Wells, *Scanning Electron Microscopy* (McGraw-Hill, New York, 1974).
[11]R. J. Young, Vacuum **44**, 353 (1993).
[12]R. Levi-Setti, T. Fox, and K. Lam, Nucl. Instrum. Methods **205**, 299 (1983).